

# Supernova prompt neutronization neutrinos and neutrino magnetic moments

Evgeny Kh. Akhmedov<sup>(a)1</sup> and Takeshi Fukuyama<sup>(b)2</sup>

<sup>(a)</sup>The Abdus Salam International Centre for Theoretical Physics  
Strada Costiera 11, I-34012 Trieste, Italy

<sup>(b)</sup>Department of Physics, Ritsumeikan University  
Kusatsu, Shiga 525-8577, Japan

## Abstract

It is shown that the combined action of spin-flavor conversions of supernova neutrinos due to the interactions of their Majorana-type transition magnetic moments with the supernova magnetic fields and flavor conversions due to the mass mixing can lead to the transformation of  $\bar{\nu}_e$  boson in the neutronization process into their antiparticles  $\nu_e$ . Such an effect would have a clear experimental signature and its observation would be a smoking gun evidence for the neutrino transition magnetic moments. It would also signify the leptonic mixing parameter  $|J_{e3}|$  in excess of  $10^{-2}$ .

---

<sup>1</sup>On leave from the National Research Centre Kurchatov Institute, Moscow, Russia. E-mail address: akhmedov@ictp.trieste.it

<sup>2</sup>E-mail address: fukuyama@se.ritsumei.ac.jp

# 1 Introduction

Type-II supernovae explosions are accompanied by copious production of neutrinos and antineutrinos which carry away about 99% of the emitted energy [1]. The supernova (SN) neutrino flux consists of two main components: a very short ( $\sim 10$  m sec) pulse of  $\bar{\nu}_e$  produced in the process of neutronization of the SN matter which is followed by a longer ( $\sim 10$  sec) pulse of thermally produced  $\nu_e, \nu_\mu, \nu_\tau$  and their antiparticles (see e.g. [1]). Neutrino mixing, the convincing evidence for which was obtained in the solar, atmospheric and reactor neutrino experiments, results in the flavor conversions of SN neutrinos in supernovae and inside the Earth (for recent discussions see, e.g., [2]). In these transitions matter enhancement of neutrino oscillations (the MSW effect [3]) plays an important role.

Since the lepton flavor is not conserved, neutrinos should possess not only mass but also flavor-off-diagonal (transition) magnetic moments  $\mu_{ab}$ , which for Majorana neutrinos are the only allowed type of magnetic moments. In transverse magnetic fields, such magnetic moments would lead to a simultaneous rotation of neutrino spin and transformation of their flavor (spin-flavor precession) [5, 6]. The neutrino spin-flavor precession can be resonantly enhanced by matter [7, 8, 9], much in the same way as matter enhances neutrino oscillations. The neutrino resonance spin-flavor precession (RSFP) in the supernova magnetic fields can lead to transmutations of different supernova neutrino species [10, 11]. For Majorana neutrinos, the possible conversions are

$$\bar{\nu}_e \rightarrow \bar{\nu}_\mu ; \bar{\nu}_\mu \rightarrow \bar{\nu}_\tau ; \bar{\nu}_\tau \rightarrow \bar{\nu}_e ; \nu_e \rightarrow \nu_\mu ; \nu_\mu \rightarrow \nu_\tau ; \nu_\tau \rightarrow \nu_e : \quad (1)$$

At the same time, matter-enhanced neutrino flavor conversions [3] lead to the transmutations

$$\bar{\nu}_e \rightarrow \bar{\nu}_\mu ; \bar{\nu}_\mu \rightarrow \bar{\nu}_\tau ; \nu_e \rightarrow \nu_\mu ; \nu_\mu \rightarrow \nu_\tau : \quad (2)$$

It is expected that the spectra of thermally produced SN neutrinos are characterized by the different mean energies [1]:

$$E_{\bar{\nu}_e} \sim 11 \text{ M eV} ; E_{\bar{\nu}_\mu} \sim 16 \text{ M eV} ; E_{\bar{\nu}_\tau} \sim E_{\nu_e} \sim E_{\nu_\mu} \sim E_{\nu_\tau} \sim 25 \text{ M eV} : \quad (3)$$

Therefore the transitions between the neutrinos of electron and non-electron flavors, whether due to the MSW effects or due to the RSFP, should modify the spectra of the SN neutrinos observed at the Earth.

Unfortunately, for thermally produced neutrinos, it is not possible to experimentally discriminate between the two effects. If, for example, electron neutrinos (or antineutrinos) are detected and their energy is found to be higher than expected, this can be due to the transition from either  $\bar{\nu}_e \rightarrow \bar{\nu}_\mu$ ; or  $\bar{\nu}_\mu \rightarrow \bar{\nu}_\tau$ ; since these initial-state neutrinos have approximately the same energies, one cannot tell whether the observed hard spectrum results from the RSFP transitions of eq. (1) or the MSW transitions of eq. (2). Analogously, if the non-electronic flavor neutrinos or antineutrinos are detected and softer than expected spectrum is observed (e.g., the spectrum of the original  $\bar{\nu}_e$ 's), this again can be due to either RSFP

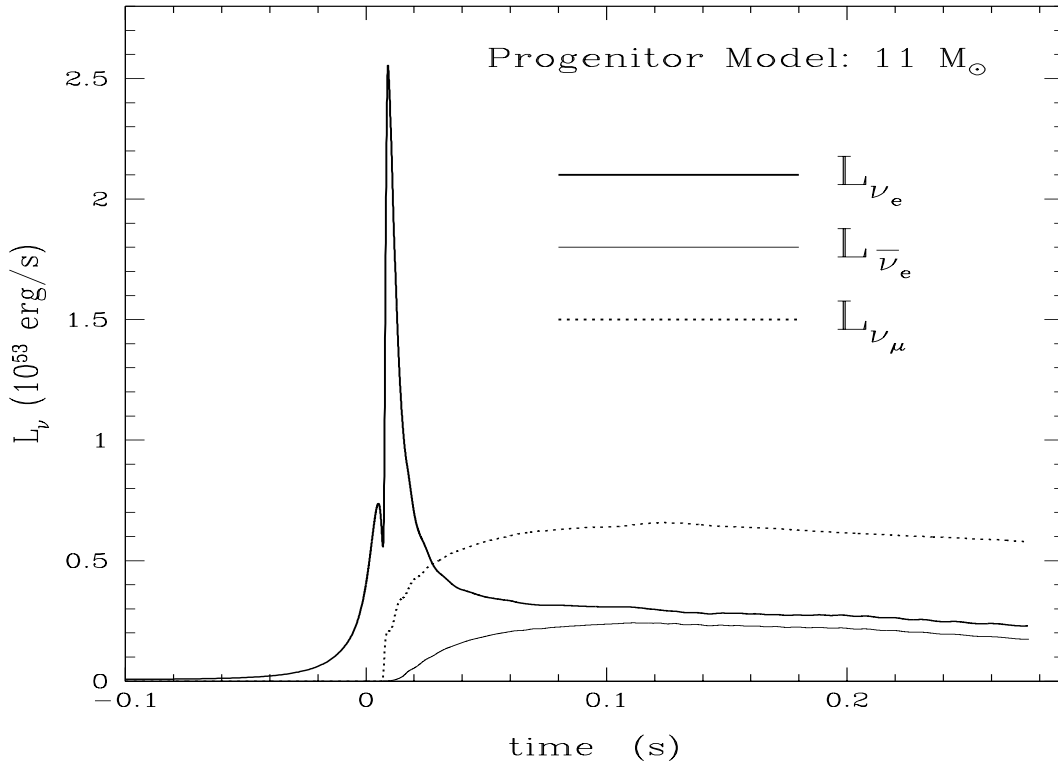


Figure 1: Luminosities of the originally produced SN neutrinos as functions of time [4].  $L_{\nu}$  stands for the collective luminosity of  $\nu_e$ ,  $\bar{\nu}_e$ , and  $\nu_{\mu}$ .

or MSW transitions. One cannot experimentally discriminate between the two possibilities because low-energy  $\nu_x$  and  $\bar{\nu}_x$  ( $x = e, \mu$ ) can only be detected via neutral-current reactions which cannot tell low energy neutrinos from antineutrinos.

The situation with the prompt neutronization neutrinos is completely different. At the neutronization stage, the emitted neutrino flux consists almost entirely of  $\bar{\nu}_e$ , the admixtures of other neutrino and antineutrino species being very small (see Fig. 1). Resonance flavor or spin-flavor conversions, acting separately, can transform these neutrinos into, e.g.,  $\nu_e$  or  $\nu_{\mu}$  respectively; as was already pointed out, one cannot discriminate experimentally between these two possibilities. However, as we discuss below, the combined action of the MSW and RSFP transitions can result in the conversion  $\bar{\nu}_e \rightarrow \nu_e$ , leading to a detectable flux of prompt neutronization neutrinos in the  $\nu_e$  channel. Electron antineutrinos can be cleanly distinguished experimentally from all the other neutrino species and in fact are the easiest to detect. Thus, such an effect would have a very clear experimental signature: a short ( $\sim 10$  m sec) pulse of  $\nu_e$  preceding the longer pulse of thermal neutrinos of all species. The detection of such a signal would constitute an unambiguous evidence for neutrino magnetic moments.

In the present paper we study the conversion of SN neutronization  $\bar{\nu}_e$  into  $\nu_e$  in the cases of the normal and inverted neutrino mass hierarchies in the full 3-flavor framework. In particular, we show that 3-flavor effects result in new spin-flavor resonances, absent in the 2-flavor approximations. We consider these resonances in detail and study their role in the  $\bar{\nu}_e \rightarrow \nu_e$  conversions in SN.

## 2 Neutrino conversions in supernovae

We assume neutrinos to be Majorana particles and consider the evolution of different neutrino species due to their flavor mixing and interaction of their transition magnetic moments with the SN magnetic fields. The neutrino evolution equation is

$$i \frac{d}{dr} \Psi = H \Psi \quad (4)$$

where  $\Psi = (\nu_e; \bar{\nu}_\mu; \bar{\nu}_\tau; \nu_e; \bar{\nu}_\mu; \bar{\nu}_\tau)^T$  is the neutrino vector of state,  $r$  is the coordinate along the neutrino trajectory and  $H$  is the effective Hamiltonian:

$$H = \begin{pmatrix} M^2=2E & B(r) \\ B(r) & M^2=2E \end{pmatrix} + V(r) \quad (5)$$

In this equation  $E$  is the neutrino energy,

$$M^2 = U \begin{pmatrix} 0 & 0 & 0 \\ 0 & m_{21}^2 & 0 \\ 0 & 0 & m_{31}^2 \end{pmatrix} U^\dagger; \quad B = \begin{pmatrix} 0 & 0 & 0 \\ 0 & B_\tau(r) & 0 \\ 0 & 0 & 0 \end{pmatrix} \quad (6)$$

where  $m_{ij}^2$  are the neutrino mass squared differences,  $U$  is the leptonic mixing matrix and  $B_\tau$  is the transverse magnetic field strength. The matrix of effective potentials

$$V = \text{diag}(V_e; V_\mu; V_e; V_\mu; V_\tau; V_\tau) \quad (7)$$

describes the coherent interactions of neutrinos of different flavor with matter. At tree level one has

$$V_e = V_\mu = \frac{p}{2G_F} (N_e - N_n = 2); \quad V_\tau = V_\nu = V_\mu = V_e = \frac{p}{2G_F} (N_n = 2); \quad (8)$$

where  $G_F$  is the Fermi constant,  $N_e$  and  $N_n$  are the electron and neutron number densities, respectively. Although the tree-level potentials of  $\nu_e$  and  $\bar{\nu}_e$  coincide, in one-loop order a difference between them arises due to the difference between the masses of the corresponding charged leptons [12]:

$$V_e = V_\mu = V_\tau + \frac{3}{2} G_F^2 m_l^2 (N_e + N_n) \ln \frac{M_W}{m} - N_e \frac{2}{3} N_n \quad (9)$$

Here  $M_W$  and  $m_l$  are the  $W$ -boson and lepton masses, respectively; for antineutrinos one has  $V = -V$ . The quantity  $V$  is very small compared to the tree-level potentials  $V_a$  ( $a = e, \mu, \tau$ ):  $V \ll 10^5 V_a$ . However, it becomes important at very high densities  $10^7 - 10^8 \text{ g/cm}^3$  [12, 2, 13].

The leptonic mixing matrix  $U$  depends on three mixing angles<sup>1</sup> which, along with the mass squared differences  $m_{21}^2$  and  $m_{31}^2$ , can be obtained from the low-energy neutrino data. For the standard parameterization of the matrix  $U$ , the analyses of the solar, atmospheric and reactor neutrino experiments yield the following allowed ranges [14]:

$$\begin{aligned} m_{21}^2 &= m_{\text{sol}}^2 = 7.1^{+1.2}_{-0.6} \cdot 10^5 \text{ eV}^2; & \tan^2 \theta_{21} &= 0.41^{+0.08}_{-0.07} \\ |m_{31}^2| &= m_{\text{atm}}^2 = 2.0^{+0.4}_{-0.3} \cdot 10^3 \text{ eV}^2; & \sin^2 2\theta_{23} &> 0.92 \\ |U_{e3}| &= \sin \theta_{13} < 0.16 \end{aligned} \quad (10)$$

The data allow two possible hierarchies (orderings) of neutrino masses, the normal hierarchy ( $m_{31}^2 > 0$ ) and inverted hierarchy ( $m_{31}^2 < 0$ ). In the case of the normal hierarchy the third mass eigenstate  $\nu_3$ , which is separated by a larger mass gap from the other two and has a small admixture of  $\nu_e$  ( $|U_{e3}|^2 \ll 1$ ), is heavier than  $\nu_1$  and  $\nu_2$ , whereas in the case of the inverted hierarchy  $\nu_3$  is the lightest mass eigenstate. The SN neutrino transmissions depend crucially on the neutrino mass hierarchy.

The density dependence of the energy levels of neutrino matter eigenstates can be read off from the effective Hamiltonian  $H$  in eq. (6) [2, 13]. It is given in Eqs. 2 and 3. At very high densities, when the potentials  $V_a$  and the potential difference  $V$  are very large, the diagonal terms in  $H$  dominate and matter eigenstates essentially coincide with the flavor eigenstates  $\nu_e, \nu_\mu$  and  $\nu_\tau$ . In the intermediate density range  $10^4 \text{ g/cm}^3 - 10^7 - 10^8 \text{ g/cm}^3$  one can neglect the potential difference  $V$  whereas  $V_a$  are still very large. In that density domain the matter eigenstates are  $\nu_e, \nu_\mu^0$  and  $\nu_\tau^0$ , where  $\nu_\mu^0$  and  $\nu_\tau^0$  are the states that diagonalize the  $\nu_\mu - \nu_\tau$  sector of the effective Hamiltonian  $H$  in vacuum. In the density region  $10^6 - 10^8 \text{ g/cm}^3$  a number of flavor and spin-flavor conversions occur (see Eqs. 2 and 3). As the matter density further decreases and approaches zero, the matter eigenstates go into the mass eigenstates  $\nu_1, \nu_2$  and  $\nu_3$ .

The resonances occur when the separation between the energy levels of neutrino matter eigenstates become minimal. In the two-flavor approximation the resonances correspond to the points where the diagonal elements of the effective Hamiltonian  $H$  become pairwise equal (level crossing points). We summarize now briefly the resonance transitions and the corresponding resonance conditions (the suffixes "H" and "L" stand for the high and low resonance densities corresponding to  $m_{31}^2$  and  $m_{21}^2$ , respectively):

<sup>1</sup>In general, it also depends on the Dirac-type CP-violating phase  $\theta_{CP}$  and two Majorana-type phases. However, the Majorana phases do not affect neutrino oscillations and spin-flavor precession; the Dirac phase does not influence the SN neutrino signal [13].

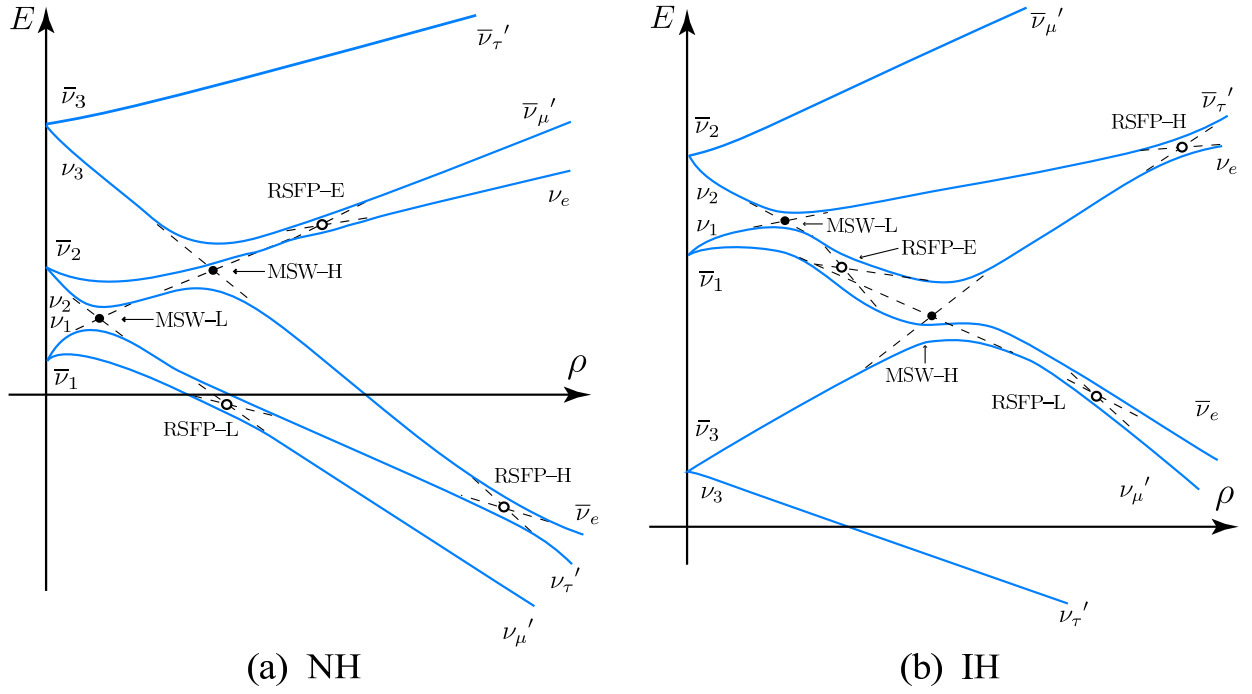


Figure 2: Neutrino energy level schemes in SN for the normal (a) and inverted (b) mass hierarchies. The case  $s_{13} > (s_{13})_c$ .

RSFP-H:  $\nu_e \leftrightarrow \nu_\mu$  (normal hierarchy);  $\nu_e \leftrightarrow \nu_\tau$  (inverted hierarchy);

$$P_{\text{res}} = \frac{1}{2G_F \frac{1}{m_N}} \frac{1}{\text{res}} (1 - 2Y_e) \frac{j m_{31}^2 j}{2E} \cos 2\theta_{13}; \quad (11)$$

RSFP-L:  $\nu_e \leftrightarrow \nu_\mu$  (normal and inverted hierarchies);

$$P_{\text{res}} = \frac{1}{2G_F \frac{1}{m_N}} \frac{1}{\text{res}} (1 - 2Y_e) \frac{m_{21}^2}{2E} \cos 2\theta_{12}; \quad (12)$$

RSFP-X:  $\nu_\mu \leftrightarrow \nu_\tau$  (normal hierarchy);  $\nu_e \leftrightarrow \nu_\tau$  (inverted hierarchy);

$$P_{\text{res}} = \frac{1}{2G_F \frac{1}{m_N}} \frac{1}{\text{res}} (1 - Y_e) \frac{j m_{31}^2 j}{2E} \cos^2 \theta_{13}; \quad (13)$$

These resonances occur when  $\sin^2 \theta_{13}$  satisfies<sup>2</sup>

$$\sin^2 \theta_{13} < \cos^2 \theta_{12} \frac{m_{21}^2}{j m_{31}^2 j} \approx 0.015; \quad (14)$$

<sup>2</sup>We use the standard notation  $s_{ij} = \sin \theta_{ij}$ ,  $c_{ij} = \cos \theta_{ij}$ .

R SFP-E :  $\nu_e \text{ } \nu_0$  (normal hierarchy);  $\nu_e \text{ } \nu_0$  (inverted hierarchy);

$$P_{\text{res}}^{\pm} \frac{1}{2G_F \frac{1}{m_N}} \frac{h}{(1-a+z)} \frac{i}{(1-a+z)^2} \frac{j m_{31}^2 j}{4a 2E} : \quad (15)$$

Here the upper and lower signs refer to the normal and inverted mass hierarchies, respectively, and

$$a = \frac{Y_e}{1-2Y_e} \frac{m_{21}^2}{j m_{31}^2} \cos 2\theta_{12}; \quad z = s_{13} \frac{Y_e}{1-2Y_e} : \quad (16)$$

The resonances occur when

$$s_{13} > (s_{13})_c \cos 2\theta_{12} \frac{m_{21}^2}{j m_{31}^2}, \quad 0.015; \quad (17)$$

which is the opposite condition to (14). Note that  $(s_{13})_c = s_{13}(a=z)$ .

M SW-H :  $\nu_e \text{ } \nu_0$  (normal hierarchy);  $\nu_e \text{ } \nu_0$  (inverted hierarchy);

$$P_{\text{res}}^{\pm} \frac{1}{2G_F \frac{1}{m_N}} \frac{j m_{31}^2 j}{2E} \cos 2\theta_{13}; \quad (18)$$

M SW-L :  $\nu_e \text{ } \nu_0$  (normal and inverted hierarchies);

$$P_{\text{res}}^{\pm} \frac{1}{2G_F \frac{1}{m_N}} \frac{j m_{31}^2 j}{2E} \cos 2\theta_{12} : \quad (19)$$

In eqs. (11) { (19)  $m_N$  is the nucleon mass and  $Y_e$  is the number of electrons per nucleon,  $Y_e = N_e/(N_e + N_n)$ . Note that the above resonances occur in the so-called isotopically neutral region of SN, where  $Y_e$  is slightly below 0.5 and very close to this value:  $1 - 2Y_e \sim 10^{-4} - 10^{-3}$ . For this reason the R SFP-H and R SFP-L resonance densities are about three orders of magnitude higher than those of the corresponding M SW resonances. Because of the smallness of  $1 - 2Y_e$ , the slopes of the energy levels of  $\nu_e, \nu_0$  and  $\nu_0$  (and also those of  $\nu_e, \nu_0$  and  $\nu_0$ ) as functions of matter density are almost identical, see figs. 2 and 3; this, in turn, leads to a number of subtle effects which we discuss below.

The spin-flavor precession resonances R SFP-H and R SFP-L have been widely discussed in the literature [10, 11]; the R SFP-X resonance was considered in ref. [10]. The R SFP-E resonances of eq. (15)<sup>3</sup> are new and considered here for the first time. They are a pure 3-flavor effect. In the 2-flavor approach, the R SFP transitions in SN between the electron-type neutrinos or antineutrinos and  $\nu_0$  ( $\bar{\nu}_0$ ) are expected to occur only in the  $\nu_e \text{ } \nu_0$  channel and to be driven by the "solar" mass squared difference  $m_{21}^2$  and mixing angle  $\theta_{12}$  [see eq. (12)]. The reason for this is that the  $\nu_e$  components in the mass eigenstates  $\nu_1$  and  $\nu_2$  are large, whereas the weight of  $\nu_e$  in the mass eigenstate  $\nu_3$  is small (equal to  $s_{13}^2$ ). However,

<sup>3</sup>The suffix "E" indicates that electron-type neutrinos are involved.

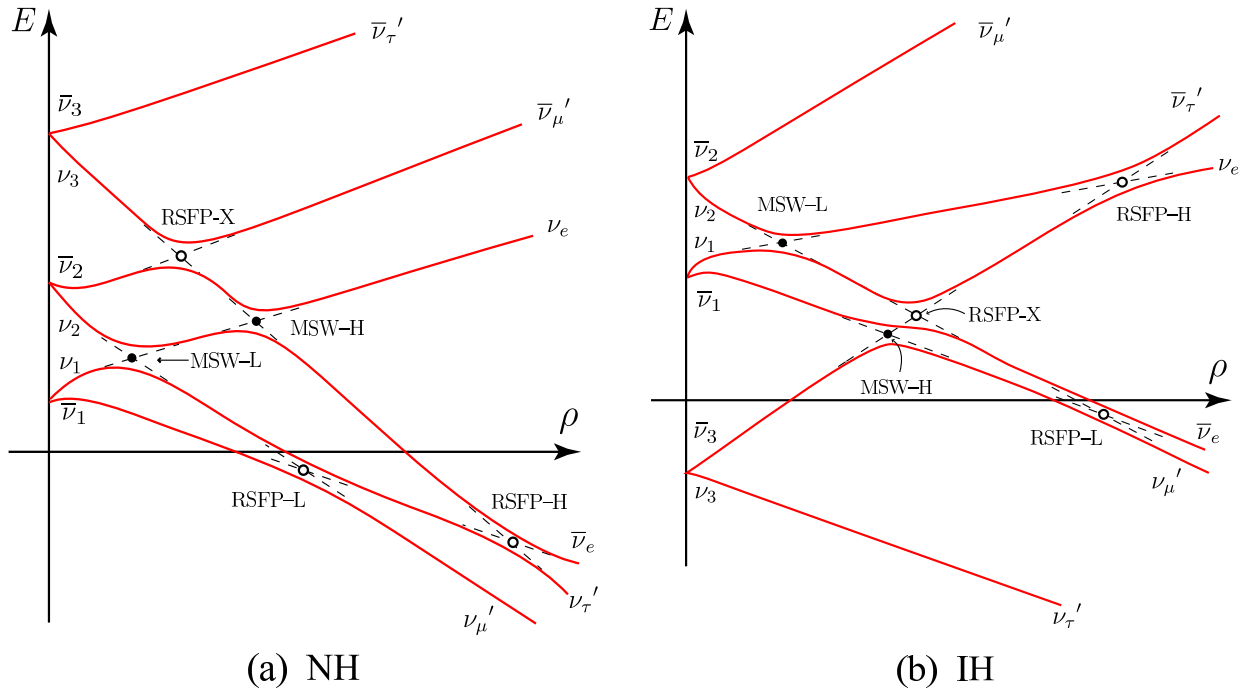


Figure 3: Neutrino energy level schemes in SN for the normal (a) and inverted (b) mass hierarchies. The case  $s_{13} < (s_{13})_c$ .

even this small weight can cause, in the case of the normal mass hierarchy, resonance  $\bar{\nu}_e \leftrightarrow \nu_e$  transitions at certain densities (see Fig. 2a). If the neutrino mass hierarchy is inverted, the RSFP-E resonance takes place in the  $\bar{\nu}_e \leftrightarrow \nu_e$  channel, but at a density which is different from the RSFP-L one and is given by eq. (15) (Fig. 2b). Thus, in that case the  $\bar{\nu}_e \leftrightarrow \nu_e$  conversions can occur in two different density regions.

We now summarize briefly the main features of the RSFP-E resonances; more detailed discussion of their properties will be given in sec. 3. The RSFP-E resonance densities (15) depend crucially on the ratio of the two small parameters,  $s_{13}^2$  and  $1 - 2Y_e$ . They also depend on both the "atmospheric" and "solar" mass squared differences  $m_{31}^2$  and  $m_{21}^2$ . The dependence on the small  $m_{21}^2$  is important since it is enhanced by the small  $1 - 2Y_e$  in the denominator of the parameter  $a$  in (16).

The RSFP-E resonances take place only when  $s_{13}$  exceeds the critical value  $(s_{13})_c$  defined in (17). In the case of the normal mass hierarchy, the RSFP-E resonance density  $(\rho_{res})_{RSFP-E}$  is larger than the MSW-H one,  $(\rho_{res})_{MSW-H}$ . With decreasing  $s_{13}$ ,  $(\rho_{res})_{RSFP-E}$  decreases and approaches  $(\rho_{res})_{MSW-H}$ ; the two densities coincide when  $s_{13} = (s_{13})_c$ .<sup>4</sup> For smaller  $s_{13}$ , in the limit  $B \rightarrow 0$  the  $\bar{\nu}_e$  level crosses the matter eigenstate level  $\bar{\nu}_{1m}$  (which coincides with

<sup>4</sup>Note that the RSFP-E resonance condition (15) is approximate; though its accuracy is very good (better than 3%), it is still not sufficient to find the critical value  $(s_{13})_c$ . The latter is obtained from a more precise resonance condition, see discussion in sec. 3.

the  $\nu_e$  level at very high densities) below the  $M_{SW}-H$  resonance point, where  $\rho_{1m}$  corresponds to  $\nu^0$  rather than to  $\nu_e$ . Thus, when  $s_{13}$  becomes smaller than  $(s_{13})_c$ , the  $R_{SFP}-E$  resonance transforms into the  $R_{SFP}-X$  one, see Fig. 3a. Similar situation takes place in the case of the inverted neutrino mass hierarchy, except that the  $R_{SFP}-E$  transition is in the  $\nu_e \leftrightarrow \nu^0$  channel, and with  $s_{13}$  decreasing and approaching  $(s_{13})_c$  from above the  $R_{SFP}-E$  resonance density increases and approaches  $(\rho_{res})_{M_{SW}-H}$  from below. The inverted hierarchy case with  $s_{13} < (s_{13})_c$  is illustrated by Fig. 3b. It should be noted that the transformation of the  $R_{SFP}-E$  resonances into the  $R_{SFP}-X$  ones with decreasing  $s_{13}$  is not sharp { due to the finite width of the resonances there is a border region where these resonances coexist. We discuss this in more detail in sec. 4.

The resonance conditions discussed above, except those for the  $R_{SFP}-E$  resonances, were found in the two-flavor approximation. This approximation is quite accurate for the  $R_{SFP}-H$ ,  $M_{SW}-H$  and  $M_{SW}-L$  resonances. For the  $R_{SFP}-L$  transitions it is sufficiently accurate when  $s_{13}$  is not too large: for  $s_{13} < 0.05$  the accuracy is better than 15%. At the same time, for  $s_{13} \sim 0.16$  which is the maximum allowed by the current data value, the 2-flavor approximation only gives the  $R_{SFP}-L$  resonance density by an order of magnitude, and full 3-flavor consideration is necessary when more precise results are needed. The sensitivity of  $(\rho_{res})_{R_{SFP}-L}$  to 3-flavor effects and in particular to the mixing parameter  $s_{13}$  is to a large extent a consequence of the above-mentioned smallness of  $1 - 2Y_e$ . It is because of this smallness that the closely situated  $\nu_e$  and  $\nu^0$  energy levels have nearly the same slope and a small variation of  $s_{13}$  or  $\theta_{31}^2$  can lead to a sizeable change in the position of their crossing point, i.e. in  $(\rho_{res})_{R_{SFP}-L}$ . The accuracy of the 2-flavor approximation is in general slightly better in the case of the inverted mass hierarchy than in the normal hierarchy case. For the  $R_{SFP}-E$  transitions, 3-flavor effects are crucial.

In addition to the above conversions, there are  $M_{SW}$  transitions governed by the effective potential difference  $V_{eff}$  and "atmospheric" mass squared difference  $m_{31}^2$ . The corresponding level crossings occur in the antineutrino channel for the normal mass hierarchy and in the neutrino channel for the inverted hierarchy. The resonance densities  $\rho_{res}$  lie in the interval  $(0; \rho_{M_{SW}})$ , their values depending on the value of  $\theta_{23}$ . The exact location of these resonances is, however, unimportant: the main role of the potential  $V_{eff}$  is to suppress the flavor mixing at high densities and convert the neutrino states  $\nu_e$  and  $\nu_\mu$  into  $\nu^0$  and  $\nu^0$  at intermediate densities. The corresponding transitions (not shown in Figs. 2 and 3) are [2, 13]:

$$\nu_e \leftrightarrow \nu^0; \quad \nu_\mu \leftrightarrow \nu^0; \quad \nu_\tau \leftrightarrow \nu^0; \quad \nu_\mu \leftrightarrow \nu_\tau \quad (\text{normal mass hierarchy}); \quad (20)$$

$$\nu_e \leftrightarrow \nu^0; \quad \nu_\mu \leftrightarrow \nu^0; \quad \nu_\tau \leftrightarrow \nu^0; \quad \nu_\mu \leftrightarrow \nu_\tau \quad (\text{inverted mass hierarchy}); \quad (21)$$

The evolution of neutrinos inside the SN can be readily followed in the adiabatic approximation (i.e. when the matter density changes slowly enough along the neutrino path). Since the flavor mixing is strongly suppressed at very high densities, neutrinos born as the flavor eigenstates  $\nu_e$ ,  $\nu_\mu$  and  $\nu_\tau$  in the supernova's core are initially in matter eigenstates. In the adiabatic regime the transitions between different matter eigenstates are strongly suppressed and so the neutrino states just follow the evolution of matter eigenstates (solid

lines in figs. 2 and 3) through a number of resonance conversions until they become mass eigenstates. If adiabaticity is strongly broken in some of the resonances, the neutrino state "hops" from the initial matter eigenstate onto the nearby one (in figs. 2 and 3, it follows the dashed line through the level crossing). In general, when the adiabaticity in the  $i$ th resonance is neither perfect nor badly broken, there are finite probabilities for the neutrino state to follow the initial matter eigenstates or to hop to another one ( $1 - P_i$  and  $P_i$ , respectively).

In each of the MSW and RSFP resonances, the hopping probability  $P_i$  is approximately given by

$$P_i \approx e^{-\gamma_i}; \quad (22)$$

where  $\gamma_i$  is the corresponding adiabaticity parameter<sup>5</sup>. For the MSW transitions one has

$$\gamma_{\text{MSW}} = \frac{\sin^2 2\theta_{ij}}{\cos 2\theta_{ij}} \frac{m_{ij}^2}{2E} L; \quad (23)$$

whereas for the RSFP-H, RSFP-L and RSFP-X transitions,

$$\gamma_{\text{RSFP}} \approx \frac{8E}{m_{ij}^2} (B_{\perp r})^2 L; \quad (24)$$

Here  $B_{\perp r}$  is the transverse magnetic field strength at the relevant RSFP resonance and  $L$  is the scale height of the effective matter density at the resonance:

$$L = \frac{1}{Y_e} \left( \frac{d(Y_e)}{dr} \right)^{-1}_{\text{res}}; \quad (25)$$

where  $Y_e = Y_e, (1 - 2Y_e)$  or  $(1 - Y_e)$ , depending on the resonance [see eqs. (11) - (19)].

The adiabaticity parameter of the RSFP-E conversion cannot in general be written in a simple form. Here we give it for the normal neutrino mass hierarchy in the limiting case  $s_{13} \ll (s_{13})_c$  which will be useful for our later discussion:

$$\gamma_{\text{RSFP-E}} \approx \frac{8E (e_0 B_{\perp r})^2}{s_{13}^2 m_{31}^2 \cos 2\theta_{12} m_{21}^2} L; \quad (26)$$

Notice that this parameter is enhanced with respect to the typical RSFP-X adiabaticity parameter (with  $e_0$  replaced by  $e$ ) by the factor

$$[s_{13}^2 \cos 2\theta_{12} (m_{21}^2 = m_{31}^2)]^{-1} \approx 10^2; \quad (27)$$

In the adiabatic regime the adiabaticity parameters satisfy  $\gamma_i \gg 1$  and the corresponding hopping probabilities  $P_i$  are strongly suppressed.

<sup>5</sup>Eq. (22) has to be modified when the relevant vacuum mixing angle is relatively large. This, however, is unimportant for our discussion.

The adiabaticity parameters depend crucially on the SN matter density and magnetic field profiles. Numerical simulations yield the SN density profiles which for  $r > 10$  km can be well approximated by

$$\rho(r) = \rho_0 \frac{(10 \text{ km})^3}{r^3}; \quad (28)$$

with  $\rho_0 \approx (1 \text{--} 15) \cdot 10^3 \text{ g/cm}^3$ . The SN magnetic field profiles are essentially unknown; in most of the studies of the SN implications of neutrino magnetic moments the profiles

$$B_\perp(r) = B_0 \frac{r_0^k}{r^k}; \quad (29)$$

with  $k = 2$  or  $3$  were assumed [10, 11]. The exponent  $k = 3$  corresponds to the dipole magnetic field, while  $k = 2$ , to the magnetic flux conservation (frozen field). We use the profile (29) with  $r_0 = 10$  km,  $k = 2$  or  $3$  and  $B_0$  a free parameter.

It is convenient to express, using eqs. (10)–(19), the adiabaticity parameters (23) and (24) in terms of the resonance densities:

$$\kappa_{MSW} \approx 55 \tan^2 \theta_{ij} Y_e \frac{\rho_0^{1-3}}{8 \cdot 10^3 \text{ g/cm}^3} \frac{\rho_{res}^{2-3}}{1 \text{ g/cm}^3}; \quad (30)$$

$$\kappa_{RSFP} \approx 3.8 \cdot 10^5 \frac{1}{Y_e} \frac{8 \cdot 10^3 \text{ g/cm}^3}{\rho_0} \frac{\rho_{res}^{\frac{2k-4}{3}}}{\rho_0} \frac{\mu_{ab}}{10^{13} \text{ B}} \frac{B_0^2}{10^{14} \text{ G}}; \quad (31)$$

Note that in the case  $k = 2$  the RSFP adiabaticity parameter does not depend on the resonance density, except possibly through the parameter  $Y_e$ .

The resonance densities of various RSFP and MSW transitions can be readily obtained from eqs. (10)–(19). For the typical SN neutrino energies  $E \approx 10 \text{--} 50$  MeV one finds

$$(\rho_{res})_{RSFP-H} \approx (0.5 \text{--} 2.5) \cdot 10^6 \text{ g/cm}^3; \quad (\rho_{res})_{RSFP-L} \approx (0.8 \text{--} 4) \cdot 10^4 \text{ g/cm}^3; \quad (32)$$

$$(\rho_{res})_{MSW-H} \approx (\rho_{res})_{RSFP-X} \approx 500 \text{--} 2500 \text{ g/cm}^3; \quad (\rho_{res})_{MSW-L} \approx 8 \text{--} 40 \text{ g/cm}^3; \quad (33)$$

For neutrino energy  $E = 15$  MeV (average energy of the neutronization  $\nu_e$ ) and normal neutrino mass hierarchy the RSFP-E resonance density varies between  $1.7 \cdot 10^3$  and  $1.3 \cdot 10^4 \text{ g/cm}^3$ , whereas for the inverted mass hierarchy it changes in the interval  $(7 \cdot 10^3 \text{--} 2 \cdot 10^5) \text{ g/cm}^3$ , depending in the value of  $s_{13}$ .

From eqs. (10) and (30) we see that the MSW-L transitions are always adiabatic, while the MSW-H ones are adiabatic for  $s_{13}^2 > 10^{-4}$  and non-adiabatic for  $s_{13}^2 < 10^{-5}$ . From eq. (31) it follows that for the RSFP transitions to be adiabatic one needs

$$\text{For } k = 2: \quad \frac{\mu_{ab}}{10^{13} \text{ B}} \frac{B_0}{10^{14} \text{ G}} > 5 \quad (\text{RSFP-H and RSFP-L}); \quad (34)$$

$$\frac{\mu_{ab}}{10^{13} \text{ B}} \frac{B_0}{10^{14} \text{ G}} > 10^2 \quad (\text{RSFP-X}); \quad (35)$$

$$\text{For } k = 3 : \quad \frac{\frac{ab}{10^{-13} B}}{\frac{B_0}{10^{14} G}} > 2 \cdot 10^3 \quad (\text{RSFP-H}) ; \quad (36)$$

$$\frac{\frac{ab}{10^{-13} B}}{\frac{B_0}{10^{14} G}} > 8 \cdot 10^3 \quad (\text{RSFP-L}) ; \quad (37)$$

$$\frac{\frac{ab}{10^{-13} B}}{\frac{B_0}{10^{14} G}} > 4 \cdot 10^5 \quad (\text{RSFP-X}) : \quad (38)$$

The adiabaticity conditions for the RSFP-E resonances depend on the resonance density, which in turn is a sensitive function of  $s_{13}$ . For the case of interest to our study, normal mass hierarchy and  $s_{13}$  ranging from  $(s_{13})_c = 0.015$  to  $(s_{13})_{\text{max}} = 0.16$ , the adiabaticity conditions for the RSFP-E resonance are

$$\frac{\frac{ab}{10^{-13} B}}{\frac{B_0}{10^{14} G}} > 4 \cdot 5 ; \quad k = 2 ; \quad (39)$$

$$\frac{\frac{ab}{10^{-13} B}}{\frac{B_0}{10^{14} G}} > (0.7 - 1) \cdot 10^6 ; \quad k = 3 ; \quad (40)$$

where we have taken into account the enhancement factor (27) and the fact that  $(\rho_{\text{res}})_{\text{RSFP-E}}$  can exceed  $(\rho_{\text{res}})_{\text{MSW-H}}$  by up to a factor of 8. Conditions (39) and (40) can be relaxed if there is an accidental partial cancellation between the two terms in square brackets in (27).

Note that for the RSFP-H transitions  $\frac{ab}{10^{-13} B} = \frac{e^0}{e^0}$ , for the RSFP-L and RSFP-E transitions  $\frac{ab}{10^{-13} B} = \frac{e^0}{e^0}$ , and for the RSFP-X ones  $\frac{ab}{10^{-13} B} = \frac{e^0}{e^0}$ .

### 3 RSFP-E conversions and overlap of resonances

The RSFP-E resonance in general takes place at densities that are not very far from that of the MSW-H resonance, and the RSFP-X resonance is always very close to the MSW-H one. For this reason in certain ranges of  $s_{13}$  some of these resonances may overlap. To study this phenomenon and also to get more insight into the nature of the RSFP-E resonance, the following approach proves to be useful. Consider the normal mass hierarchy case (the inverted hierarchy case is analyzed quite analogously). We note that in the vicinity of the MSW-H resonance the energy levels of  $e$ ,  $\nu^0$  and  $\nu^0$  are close to each other, whereas the other three energy levels are rather far. In this region one can therefore neglect the influence of the far-lying states and consider the evolution of  $e$ ,  $\nu^0$  and  $\nu^0$  separately. The corresponding approximate evolution equation is

$$i \frac{d}{dr} \begin{pmatrix} \nu^0 \\ e \\ \nu^0 \end{pmatrix} = \begin{pmatrix} 1 & 0 & 0 \\ 0 & A & 0 \\ 0 & 0 & 0 \end{pmatrix} + \begin{pmatrix} s_{12}^2 + s_{13}^2 + V_e & s_{13} c_{13} & 0 \\ s_{13} c_{13} & c_{13}^2 + V_e & 0 \\ e^0 B_? & B_? & c_{12}^2 + V_e \end{pmatrix} \begin{pmatrix} \nu^0 \\ e \\ \nu^0 \end{pmatrix} ; \quad (41)$$

where  $m_{31}^2 = 2E$  and  $m_{21}^2 = 2E$ . For small  $B_?$  the characteristic equation of the effective Hamiltonian on the r.h.s. of eq. (41) can be readily solved (note that  $\nu^0$  decouples

in the limit  $B \rightarrow 0$ , and the solutions give the energy levels of matter eigenstates:

$$E_{1m,2m} = \frac{1}{2} (V_e + V + s_{12}^2) \pm \sqrt{(\cos 2\theta_{13} (V_e + V) + s_{12}^2)^2 + \sin^2 2\theta_{13} \Delta^2};$$

$$E_{3m} = c_{12}^2 V; \quad (42)$$

We have checked numerically that this approximation is extremely good, and for most densities the obtained eigenvalues coincide with those of the full (3+3)-state problem to an accuracy better than 1%.

The MSW-H resonance corresponds to the avoided level crossing of the first and second eigenvalues; the resonance density is obtained from the condition that the term in brackets under the square root in  $E_{1m,2m}$  vanishes, which yields

$$P \frac{1}{2G_F} \frac{1}{m_N} \text{res} Y_e = \cos 2\theta_{13} s_{12}^2 \quad (\text{MSW-H}); \quad (43)$$

This equation corrects the 2-flavor resonance condition (18). There is one more level crossing described by eq. (41) (that of the first and third eigenvalues (it becomes an avoided level crossing when the magnetic field is switched on)). The physical interpretation of this level crossing depends on where it takes place. If it occurs at  $\rho > (\rho_{\text{res}})_{\text{MSW-H}}$ , the crossing is on the branch of the first eigenvalue  $E_{1m}$  that corresponds to  $\nu_e$ , i.e. it describes the RSFP-E resonance  $\nu_e \leftrightarrow \nu_\mu$  (see eq. 2a). If, however, the crossing occurs at  $\rho < (\rho_{\text{res}})_{\text{MSW-H}}$ , the resonance point lies on the branch of  $E_{1m}$  corresponding to  $\nu_\mu$ . In this case it describes the RSFP-X resonance  $\nu_\mu \leftrightarrow \nu_\tau$  (eq. 3a). The position of the crossing point depends on the value of  $s_{13}$ . There is the critical value  $(s_{13})_c$  for which it occurs at  $\rho = (\rho_{\text{res}})_{\text{MSW-H}}$  and which delineates the two possibilities: For  $s_{13} < (s_{13})_c$  there is the RSFP-X resonance, whereas for  $s_{13} > (s_{13})_c$  the RSFP-E resonance occurs. The critical value  $(s_{13})_c$  can be found from eqs. (42) and (43) and is approximately given in (17).

The RSFP-E resonance condition (15) is obtained by expanding the eigenvalues (42) in small parameters  $\Delta^2$  and  $\theta_{13}$ ; note, however, that  $(s_{13})_c$  cannot be found from the lowest order expansion (15) and a more accurate expression has to be used. With  $s_{13}$  varying between  $(s_{13})_c \approx 0.015$  and 0.16, the RSFP-E resonance density  $\rho_{\text{RSFP-E}}$  changes from  $\rho_{\text{MSW-H}} \approx 1.7 \cdot 10^8 \text{ g/cm}^3$  to  $1.3 \cdot 10^4 \text{ g/cm}^3$  (for neutrino energy  $E = 15 \text{ MeV}$ ).

The RSFP-X resonance density is in general very close to that of the MSW-H resonance: for  $s_{13} = (s_{13})_c$  the two resonance densities coincide, whereas for  $s_{13} < (s_{13})_c$  the RSFP-X resonance density is given by

$$P \frac{1}{2G_F} \frac{1}{m_N} \text{res} (1 - Y_e) \approx c_{13}^2 - c_{12}^2 \quad (\text{RSFP-X}); \quad (44)$$

This expression corrects the 2-flavor result (13).

Let us now consider the cases of possible overlap of the resonances. From eqs. (42) and (43) we find that when the RSFP-E and MSW-H (or RSFP-X and MSW-H) resonances are close to each other their densities satisfy

$$\frac{j_i}{s_{13}} \frac{M_{SW-H}}{H}, \quad s_{13}^2 > (s_{13})_c^2 - \frac{1}{\cos^2 \theta_{12}} = \frac{j_{13}^2 (s_{13})_c^2}{(s_{13})_c}; \quad (45)$$

where  $i = \text{RSFP-E}$  for  $s_{13} > (s_{13})_c$  and  $i = \text{RSFP-X}$  for  $s_{13} < (s_{13})_c$ . The condition of no overlap between the MSW-H and RSFP-X resonances can be written as [15, 16]

$$\tan 2\theta_{13} (\text{res})_{MSW-H} + \frac{2}{m_{31}^2} \frac{B_{\nu\tau}}{2E} (\text{res})_{RSFP-X} < (\text{res})_{MSW-H} - (\text{res})_{RSFP-X}; \quad (46)$$

and similar condition can be written for the MSW-H and RSFP-E resonances. To find out when the no-overlap conditions are satisfied, let us assume that the RSFP-X and RSFP-E resonance widths are small compared to the width of the MSW-H resonance, so that the second term on the l.h.s. of eq. (46) (and the corresponding term in the no-overlap condition of the MSW-H and RSFP-E resonances) can be neglected. Then from (46) and (45) we find that the conditions of no overlap become

$$\frac{s_{13}}{(s_{13})_c} > \frac{P_{21}}{2 + 1'} \approx 2.4; \quad (\text{MSW-H and RSFP-E}); \quad (47)$$

$$\frac{s_{13}}{(s_{13})_c} < \frac{P_{21}}{2 - 1'} \approx 0.41; \quad (\text{MSW-H and RSFP-X}); \quad (48)$$

Thus, the RSFP-E and MSW-H (or RSFP-X and MSW-H) resonances overlap when  $s_{13}$  is within a factor of 2.4 of the critical value  $(s_{13})_c \approx 0.015$  and do not overlap in the opposite case.

## 4 $\nu_e \rightarrow \nu_e$ conversions of neutronization neutrinos

Consider now the transformations experienced by the neutronization  $\nu_e$  as they propagate from the supernova's core outwards

(a) Normal mass hierarchy. In this case the  $\nu_e \rightarrow \nu_e$  conversion is driven by the RSFP-E resonance or by an interplay of the MSW-H and RSFP-X resonances, depending on the value of  $s_{13}$ . Let us first consider the case  $s_{13} > (s_{13})_c \approx 0.015$ . The neutronization  $\nu_e$  first encounter the RSFP-E resonance and, if the resonance transition is adiabatic, get converted into  $\nu^0$  (see g. 2a). As these  $\nu^0$  propagate towards the region of very small matter densities, they transform into the mass eigenstate  $\nu_2$ , which contains the  $\nu_e$  component with the weight  $s_{12}^2$ . Thus, for  $s_{13} > (s_{13})_c$  the  $\nu_e \rightarrow \nu_e$  conversion probability is

$$P(\nu_e \rightarrow \nu_e) = (1 - P_{RSFP-E}) s_{12}^2; \quad (49)$$

In deriving this formula we have assumed that  $s_{13}$  is not too close to  $(s_{13})_c$ , so that condition (47) is satisfied and the RSFP-E and MSW-H resonances do not overlap. We shall consider the case of the overlapping resonances below.

In the case  $s_{13} < (s_{13})_c \approx 0.015$ , the RSFP-E resonance does not exist; the neutronization  $\bar{\nu}_e$  born in the core of the star and moving outwards first encounter the MSW-H resonance and then the RSFP-X resonance (see fig. 3a). Let us first consider the case when these resonances do not overlap; the neutrino conversions in them can then be treated as independent. At the MSW-H resonance the neutronization  $\bar{\nu}_e$  get converted into  $\bar{\nu}_\mu$ , the efficiency of the transition depending on its degree of adiabaticity. The produced  $\bar{\nu}_\mu$  can then be transformed into  $\bar{\nu}_\tau$  in the RSFP-X resonance (see fig. 2a). As these  $\bar{\nu}_\tau$  propagate further towards small density regions, they transform into the mass eigenstate  $\bar{\nu}_2$ . Thus, in this case the  $\bar{\nu}_e \rightarrow \bar{\nu}_\tau$  conversion probability is

$$P(\bar{\nu}_e \rightarrow \bar{\nu}_\tau) = (1 - P_{MSW-H})(1 - P_{RSFP-X})s_{12}^2 : \quad (50)$$

The no-overlap condition (48) implies  $s_{13}^2 < [(s_{13})_c = 2.41]^2 \approx 4 \times 10^{-5}$ . This means that the MSW-H resonance is in fact non-adiabatic or moderately non-adiabatic. For the average energy of the neutronization neutrinos  $\bar{E} \approx 15$  MeV, from eqs. (18), (30) and (22) one finds  $(1 - P_{MSW-H}) \approx 0.6$ , and so the probability  $P(\bar{\nu}_e \rightarrow \bar{\nu}_\tau) \approx 0.18$ .

Let us now consider the case of overlapping resonances. It is instructive to calculate the  $\bar{\nu}_e \rightarrow \bar{\nu}_\tau$  conversion probability in perturbation theory. Strictly speaking, this approach is only justified when  $P(\bar{\nu}_e \rightarrow \bar{\nu}_\tau) \ll 1$ ; however, it gives the correct order-of-magnitude estimate even if this quantity is not too small. Moreover, it allows an exponentiation procedure which is expected to give the correct result in a wide range of values of  $P(\bar{\nu}_e \rightarrow \bar{\nu}_\tau)$ . Another advantage of this method is that it is operative in both the overlapping and non-overlapping resonance cases and allows one to study the smooth transition from the RSFP-E-mediated  $\bar{\nu}_e \rightarrow \bar{\nu}_\tau$  transition to that occurring through the combination of the MSW-H and RSFP-X resonances.

We shall make use of the evolution equation (41). Direct integration yields the following expression for the amplitude  $\bar{\nu}_\tau$ :

$$\bar{\nu}_\tau(r) = (i) \int_0^r dr^0 [ \bar{\nu}_e \rightarrow \bar{\nu}_\tau(r^0) + \bar{\nu}_\mu \rightarrow \bar{\nu}_\tau(r^0) ] B_{\tau}^{\tau}(r^0) e^{(i) \int_0^{R_{r^0}} dr_1 (c_{12}^2 - v)} : \quad (51)$$

Here the amplitudes  $\bar{\nu}_e(r)$  and  $\bar{\nu}_\mu(r)$  have to be found from the same system of equations (41). In perturbation theory one considers the  $\bar{\nu}_\tau$  amplitude in the lowest order in magnetic field, i.e. neglects the effects of the magnetic field on  $\bar{\nu}_e(r)$  and  $\bar{\nu}_\mu(r)$ . The equation for  $\bar{\nu}_\tau(r)$  then decouples from the rest of the system, and the amplitudes  $\bar{\nu}_e(r)$  and  $\bar{\nu}_\mu(r)$  can

be readily found, e.g., in the adiabatic approximation<sup>6</sup>. Eq. (51) then gives

$$P_{e \rightarrow \mu}^0(r) = \left( \frac{1}{2} \right) \int_{r_0}^r dr^0 [e^{i g^0(r^0)} + c(r^0)] B_{\mu}^0(r^0) e^{-i g^0(r^0)}; \quad (52)$$

Here

$$g^0(r) = \int_{r_0}^r dr_1 [E_{1m}(r_1) - \frac{1}{2} \Delta_{22}^2 + V(r_1)]; \quad (53)$$

and  $s(r)$  and  $c(r)$  are sine and cosine of the mixing angle  $\theta_m(r)$  defined through

$$\tan 2\theta_m(r) = \frac{\sin 2\theta_{13}}{\cos 2\theta_{13} - \frac{s_{12}^2}{s_{22}^2} [V_e(r) - V(r)]}; \quad (54)$$

At the MSW-H resonance point,  $\theta_m = 45^\circ$ ; at much higher densities  $\theta_m \rightarrow 0$ , while at densities much lower than the MSW-H resonance one,  $\theta_m \rightarrow 90^\circ$ .

The phase factor  $e^{i g^0(r)}$  in the integrand of (52) is a fast oscillating function for all  $r$  except in the vicinity of the stationary phase point  $r_0$  at which  $g^0(r_0) = 0$ ; the integral therefore receives its main contribution from the neighbourhood of this point and can be evaluated in the stationary phase approximation. This gives, up to an unimportant phase factor,

$$P_{e \rightarrow \mu}^0 \approx \frac{1}{2} \frac{1}{|g^0(r_0)|} [e^{i g^0(r_0)} + c(r_0)] B_{\mu}^0(r_0); \quad (55)$$

where the calculated amplitude  $P_{e \rightarrow \mu}^0$  corresponds to large enough values of coordinate, so that the neutrinos have already passed through the MSW-H and RSFP-E or RSFP-X resonances. The probability of the  $\nu_e \rightarrow \nu_e$  conversion is then

$$P(\nu_e \rightarrow \nu_e) = P(\nu_e \rightarrow \nu_e)^0 s_{12}^2 = \frac{1}{2} s_{12}^2; \quad (56)$$

From eqs. (53) and (42) one can see that the stationary phase condition  $g^0(r_0) = 0$  coincides with the condition of crossing of the first and third eigenvalues of the effective Hamiltonian in (41). Thus, the stationary phase point is just the level crossing point that defines the positions of the RSFP-E or RSFP-X resonances, depending on whether the crossing occurs above or below the MSW-H resonance density. Using the stationary phase condition  $g^0(r_0) = E_{1m}(r_0) - E_{3m}(r_0) = 0$ , one can readily find  $g^0(r_0)$ :

$$g^0(r_0) \approx 2V_e \frac{s_{13}^2 \cos 2\theta_{12}}{(s_{12}^2 - 2s_{22}^2)} \frac{1}{2V_e} L^{-1}; \quad (57)$$

Here we have taken into account that  $Y_e \approx 1=2$ .

<sup>6</sup>This approximation is good in the case of overlapping MSW-H and RSFP-X resonances, and also in all cases when the RSFP-E resonance transition takes place. The method can be easily modified to include possible deviations from adiabaticity.

Consider first the case  $s_{13} = (s_{13})_c = (s_{13})_c$ . This gives  $(r_0)_{MSW-H}$ , i.e.  $2V_e(r_0)$ . From eq. (57) we then find

$$g^0(r_0) = L^{-1} (s_{13}^2 \cos 2\theta_{12}) : \quad (58)$$

Substituting this into eq. (55) one obtains

$$P(e \rightarrow 0) = j^0 j^2 \frac{4 [e^{-i} B_2(r_0)]^2}{2 s_{13}^2 \cos 2\theta_{12}} L ; \quad (59)$$

where we have taken into account that for  $(r_0)_{MSW-H}$  one has  $s(r_0) = 1$ ,  $c(r_0) = 0$ . Notice that this expression coincides with  $(=2)_{RSFP-E}$  where  $(=2)_{RSFP-E}$  was defined in eq. (26). Thus, the  $e \rightarrow 0$  conversion in this case is driven by the RSFP-E resonance. It is interesting to note that the perturbation-theoretic expression (59) is just the first term in the expansion of the transition probability  $P(e \rightarrow 0) = 1 - \exp[-(=2)_{RSFP-E}]$  in the small  $(=2)_{RSFP-E}$  limit. Thus, eq. (59) is in accord with eqs. (49) and (56).

Let us now consider the case  $s_{13} = (s_{13})_c$ . In this case  $(r_0)$  coincides with the small- $s_{13}$  limit of  $(=2)_{RSFP-X}$  given in eq. (44). Using this condition we find from (57)

$$g^0(r_0) = L^{-1} (c_{13}^2 - c_{12}^2) : \quad (60)$$

Substituting this into eq. (55) yields

$$P(e \rightarrow 0) = j^0 j^2 \frac{4 [e^{-i} B_2(r_0)]^2}{2 c_{13}^2 - c_{12}^2} L ; \quad (61)$$

where we have taken into account that for densities below  $(=2)_{MSW-H}$  and outside the RSFP-H resonance region one has  $s(r_0) = 0$ ,  $c(r_0) = 1$ . We note that this expression coincides with  $(=2)_{RSFP-X}$ . Thus, the  $e \rightarrow 0$  conversion in this case is driven by the combination of the MSW-H and RSFP-X resonances and goes through the chain of transitions  $e \rightarrow 0 \rightarrow 0$ . Eq. (61) gives the first term in the expansion of the transition probability

$$P(e \rightarrow 0) = (1 - e^{-2(=2)_{MSW-H}}) (1 - e^{-2(=2)_{RSFP-X}}) \quad (62)$$

in small  $(=2)_{RSFP-X}$  (note that in our case the first factor in (62) is equal to unity since we assume the MSW-H transition to be adiabatic). Thus, eq. (61) agrees with eqs. (50) and (56).

We have considered the cases when the stationary point is situated above or below the MSW-H resonance point and sufficiently far from it. We found that in those cases the  $e \rightarrow 0$  transition is driven either by the RSFP-E resonance or by the sequence of the MSW-H and RSFP-X resonances, as the resonance regions do not overlap. When  $s_{13} = (s_{13})_c$ , the stationary phase point is close to the MSW-H resonance one, which leads to the overlap of the resonances. In that case the transition mechanism is a subtle interplay of both the mechanisms discussed above. In particular, when  $s_{13} = (s_{13})_c$  one has  $s(r_0) = c(r_0) = 1 = \frac{1}{\sqrt{2}}$ ,

and the magnetic moments  $\mu_e$  and  $\mu_\nu$  enter into the amplitude  $A_{e\nu}$  in eq. (55) with equal weights. This corresponds to the maximal interference of the two mechanisms discussed above; the interference can be either constructive or destructive, depending on the relative sign of  $\mu_e$  and  $\mu_\nu$ . When  $s_{13} \neq (s_{13})_c$  but not exactly equal to this critical value, the direct  $\nu_e \rightarrow \nu_\mu$  conversion due to the RSFP-E resonance and the  $\nu_e \rightarrow \nu_\mu \rightarrow \nu_\tau$  transitions due to the combined action of the MSW-H and RSFP-X resonances give comparable contributions to  $P(\nu_e \rightarrow \nu_\mu)$ . The relative weight of these contributions depends on the value of the mixing angle  $\theta_m$  at the level crossing point  $r_0$ .

We have found that in the cases of non-overlapping resonances the perturbation-theoretic expressions for the probability  $P(\nu_e \rightarrow \nu_\mu)$  are just the first-order terms in the expansions of the expressions of the type  $(1 - \exp[-(\Delta E)^{-1}])$ . It is therefore natural to assume that this is also true in general, and the probability  $P(\nu_e \rightarrow \nu_\mu)$  can be found from (55) by the exponentiation procedure. According to this procedure, the probability  $P(\nu_e \rightarrow \nu_\mu)$  is obtained as

$$P(\nu_e \rightarrow \nu_\mu) = 1 - e^{-\bar{g}}; \quad (63)$$

where

$$\bar{g} = \frac{4}{|g^0(r_0)|} [|\mu_e \mu_\nu| s(r_0) + c(r_0)]^2 B_{\nu_e}(r_0)^2 \quad (64)$$

with  $g^0(r_0)$  defined in eq. (57). Eqs. (63), (64) are expected to be valid for all values of  $\theta_m$ , not necessarily  $\theta_m = 1$ , provided that the MSW-H resonance conversion is adiabatic. The probability of the  $\nu_e \rightarrow \nu_\mu$  conversion we are interested in is then found from eq. (56).

As can be seen from eqs. (49), (50) and (56), in the case of the normal neutrino mass hierarchy the maximum possible value of  $P(\nu_e \rightarrow \nu_\mu)$  is  $s_{12}^2 \approx 0.3$ .

(b) Inverted mass hierarchy. In this case the neutrinoization  $\nu_e$  first encounter the RSFP-H resonance and get converted into  $\nu_\mu$ . The destiny of the latter depends on whether  $s_{13}$  is above or below the critical value  $(s_{13})_c$  (see figs. 2b and 3b).

Let us first consider the case  $s_{13} > (s_{13})_c$ . The  $\nu_\mu$  that emerge from the RSFP-H resonance next reach the MSW-H resonance and get converted into  $\nu_e$ , which then encounter the RSFP-E resonance where they can be transformed into  $\nu_\tau$  (fig. 2b). If this latter conversion occurs, the neutrinoization  $\nu_e$  end up as neutrinos and not antineutrinos (in general, for a  $\nu_a \rightarrow \nu_b$  conversion, neutrinos should experience an odd number of the RSFP transformations). Therefore the  $\nu_e \rightarrow \nu_\mu$  transition we are interested in takes place only if the RSFP-E resonance is non-adiabatic. Then  $\nu_e$  emerging from the MSW-H resonance pass through the RSFP-E resonance unaffected. As they propagate towards very small densities, they transform into  $\nu_1$ , which have the  $\nu_e$  component with the weight  $c_{12}^2$ . Thus, the  $\nu_e \rightarrow \nu_\mu$  conversion occurs through the sequence of transitions  $\nu_e \rightarrow \nu_\mu \rightarrow \nu_e \rightarrow \nu_1$ , and its probability is

$$P(\nu_e \rightarrow \nu_\mu) = (1 - P_{\text{RSFP-H}})(1 - P_{\text{MSW-H}})P_{\text{RSFP-E}}c_{12}^2; \quad (65)$$

In the case  $s_{13} < (s_{13})_c$ , the  $\nu_\mu$  emerging from the RSFP-H resonance next reach the

R SFP-X resonance and can be converted there into  $\nu_0$  ( g. 3b). For the  $\nu_e \rightarrow \nu_e$  transition to occur, this resonance has to be non-adiabatic. Then  $\nu_0$  pass through the R SFP-X resonance unscathed and propagate towards the M SW-H resonance where, as in the case  $s_{13} > (s_{13})_c$ , they can be converted into  $\nu_e$ . These  $\nu_e$  subsequently transform into  $\nu_1$  in the small density regions. The sequence of transitions in this case is therefore the same as in the case  $s_{13} > (s_{13})_c$ . The probability of the  $\nu_e \rightarrow \nu_e$  conversion is

$$P(\nu_e \rightarrow \nu_e) = (1 - P_{\text{RSFP-H}})(1 - P_{\text{MSW-H}})P_{\text{RSFP-X}} c_{12}^2 : \quad (66)$$

Note that in the case  $s_{13} < (s_{13})_c$ , the M SW-H resonance transition is adiabatic only for  $s_{13}$  relatively close to  $(s_{13})_c$ .

As can be seen from eqs. (65) and (66), in the case of the inverted neutrino mass hierarchy the maximum possible value of  $P(\nu_e \rightarrow \nu_e)$  is  $c_{12}^2 \approx 0.7$ .

## 5 Discussion

We have considered neutrino flavor and spin-flavor transitions in supernovae in the full 3-flavor framework and found that, in addition to the known MSW and R SFP resonances that can be obtained assuming the transitions to be approximately 2-flavor ones, there are new R SFP resonances which are pure 3-flavor effects and cannot be found in 2-flavor approximations. We have studied these new resonances and their interplay with the other nearby resonances in some detail, including the case of overlapping resonances. We have explored the role of these resonances in the transformation of neutronization  $\nu_e$  into their antiparticles. It was found that such transformations depend crucially on the value of the neutrino mixing parameter  $s_{13}$  and are in general possible for both normal and inverted neutrino mass hierarchies. We obtained the relevant transition probabilities in each case.

Let us discuss now the conditions on neutrino magnetic moments and SN magnetic fields that have to be satisfied in order for the  $\nu_e \rightarrow \nu_e$  transitions of the neutronization neutrinos to be efficient. In the case of the normal neutrino mass hierarchy the  $\nu_e \rightarrow \nu_e$  transition probabilities are given by eqs. (49) and (50) for  $s_{13} > (s_{13})_c$  and  $s_{13} < (s_{13})_c$  respectively. For  $s_{13} > (s_{13})_c$  the efficiency of the  $\nu_e \rightarrow \nu_e$  conversion is determined by the R SFP-E adiabaticity parameter, eq. (26). Assuming the power-law magnetic field profile (29), we find from eqs. (39) and (40) that in the case  $B_0 = 10^{14}$  G and  $k = 2$  the transition is adiabatic ( $P_{\text{RSFP-E}} > 1$ ) if  $\mu_{e0} > 5 \cdot 10^{13} \mu_B$ , while for the exponent  $k = 3$  this would require  $\mu_{e0} > 10^9 \mu_B$ , a value already experimentally excluded. Note that magnetic fields as strong as  $10^{16}$  G have been considered possible in supernovae [17]; if this is the case, for  $k = 3$  the transition magnetic moments  $\mu_{e0} \approx 10^{11} \mu_B$  would cause strong  $\nu_e \rightarrow \nu_e$  conversions, while for  $k = 2$  magnetic moments as small as  $5 \cdot 10^{15} \mu_B$  would do.

For  $s_{13} < (s_{13})_c$  the  $\nu_e \rightarrow \nu_e$  conversion is driven by a combination of the MSW-H and R SFP-X resonance transitions. For values of  $s_{13}$  only slightly below the critical value, the transition efficiency is mainly determined by the R SFP-X adiabaticity parameter. From

eqs. (35) and (38) we find that in the case  $B_0 = 10^{14}$  G and  $k = 2$  the RSFP-X transition is adiabatic if  $\beta > 10^{11} B$ , while for the exponent  $k = 3$  this would require  $\beta > 4 \cdot 10^8 B$ . For different values of  $B_0$  these limits would have to be rescaled accordingly.

In the case of the inverted neutrino mass hierarchy the  $\nu_e \rightarrow \nu_e$  transition probabilities are given by eqs. (65) and (66) for  $s_{13} > (s_{13})_c$  and  $s_{13} < (s_{13})_c$  respectively. If the MSW-H transition is adiabatic, the  $\nu_e \rightarrow \nu_e$  conversion probability is determined by the RSFP-H adiabaticity parameter  $\kappa_{\text{RSFP-H}}$ . From eqs. (34) and (36) we find that for  $B_0 = 10^{14}$  G and  $k = 2$  the transition is adiabatic if  $\beta > 5 \cdot 10^{13} B$ , while for the exponent  $k = 3$  the adiabaticity of the transition would require  $\beta > 2 \cdot 10^{10} B$ . These conditions are comparable with the conditions we obtained for  $\nu_e \rightarrow \nu_e$  in the case of the normal neutrino mass hierarchy and  $s_{13} > (s_{13})_c$ . From eqs. (65) and (66) it follows that in the inverted hierarchy case the  $\nu_e \rightarrow \nu_e$  transitions can only be efficient if the RSFP-X transition [for  $s_{13} < (s_{13})_c$ ] or RSFP-E transition [for  $s_{13} > (s_{13})_c$ ] is non-adiabatic. It is easy to see that these conditions can be satisfied without any conflict with the requirement of the adiabaticity of the RSFP-H condition.

It might also be useful to give the conditions for the efficient  $\nu_e \rightarrow \nu_e$  transitions of the neutronization neutrinos directly in terms of the SN magnetic field strength at the resonance, i.e. independently of the supernova magnetic field model. In the case of the normal neutrino mass hierarchy and  $s_{13} > (s_{13})_c$ , the requirement that the RSFP-E adiabaticity parameter exceeds unity yields  $\beta > 10^{13} B \approx 1.5 \cdot 10^9$  G. For the normal hierarchy and  $s_{13}$  slightly below the critical value  $(s_{13})_c$ , the condition  $\kappa_{\text{RSFP-X}} > 1$  leads to  $\beta > 10^{13} B \approx 1.5 \cdot 10^9$  G. In the case of the inverted neutrino mass hierarchy the  $\nu_e \rightarrow \nu_e$  transitions can only be efficient when  $\kappa_{\text{RSFP-H}} > 1$ , which yields  $\beta > 10^{13} B \approx 1.2 \cdot 10^9$  G.

Thus, we have seen that in both cases of the normal and inverted neutrino mass hierarchies sizeable  $\nu_e \rightarrow \nu_e$  transitions of the SN neutronization neutrinos are in general possible<sup>7</sup>. In the normal hierarchy case, the maximum possible transition probability is equal to  $s_{12}^2 \approx 0.3$ , whereas for the inverted hierarchy it is  $c_{12}^2 \approx 0.7$ . Thus, in the inverted hierarchy case the  $\nu_e \rightarrow \nu_e$  conversion probability can be higher. In both cases the  $\nu_e \rightarrow \nu_e$  conversion occurs only when  $s_{13}$  is not too small: For the RSFP-E driven transitions, one needs  $s_{13} > (s_{13})_c \approx 0.015$  for the RSFP-E resonance to exist; for the transitions occurring through the combinations of the MSW-H and RSFP-X resonances or RSFP-H and MSW-H resonances, one needs  $s_{13} \gtrsim 10^{-2}$  for the MSW-H resonance to be adiabatic.

Conversion of the SN neutronization  $\nu_e$  into  $\nu_e$  would have a very clear and distinct experimental signature, especially in water Cherenkov detectors. We will consider the Super-Kamiokande detector (total volume 32 kt) as an example. For a galactic supernova at 10 kpc from the Earth, one expects in this detector about 12 events from the detection of the neutronization  $\nu_e$  through the  $\nu_e \nu_e \rightarrow \nu_e \nu_e$  scattering reaction, assuming no flavor or spin-

<sup>7</sup>SN neutrinos could also experience  $\nu_e \rightarrow \nu_e$  transitions due to neutrino decay into a lighter (anti)neutrino and Majoron. This, however, would lead to a significant degradation of the neutrino energy, and so the  $\nu_e \rightarrow \nu_e$  conversion due to the neutrino transition magnetic moments can be clearly distinguished experimentally from that caused by neutrino decay.

flavor conversions (see e.g. 22 in [4]). These events should occur in a very short time interval of  $(10 \text{--} 20)$  ms and should precede a longer signal of neutrinos and antineutrinos of all flavors. If the  $\nu_e \rightarrow \bar{\nu}_e$  conversion occurs, the neutronization burst observed by terrestrial detectors should contain a significant fraction of electron antineutrinos, up to 30% in the normal hierarchy case and up to 70% in the case of the inverted mass hierarchy. The main detection mechanism of  $\bar{\nu}_e$  is through the  $\bar{\nu}_e p \rightarrow n e^+$  reaction, which has a much larger cross section than that of  $\bar{\nu}_e e$  scattering: at the average energy of the neutronization neutrinos  $E \approx 15$  MeV one has  $(\bar{\nu}_e p \rightarrow n e^+) = (\bar{\nu}_e e \rightarrow \bar{\nu}_e e) \approx 150$ . Therefore one can expect a very strong signal of  $\bar{\nu}_e$  { up to 1200 (500) events in the case of the normal (inverted) mass hierarchy } in a very short time interval of  $(10 \text{--} 20)$  ms. Note that  $\bar{\nu}_e$  can be cleanly distinguished experimentally from all other neutrino and antineutrino species [18].

Supernova neutronization  $\bar{\nu}_e$  can also be observed in the SNO detector, which contains about 1.4 kt of light water in addition to 1 kt of heavy water. The  $\bar{\nu}_e p \rightarrow n e^+$  capture reaction in light water can result in up to 50 (20) events in the case of the normal (inverted) neutrino mass hierarchy. Detection of the neutronization  $\bar{\nu}_e$  through the charged-current reaction  $\bar{\nu}_e d \rightarrow n n e^+$  in heavy water is not of much interest since the cross section of this process is much smaller than that of the  $\bar{\nu}_e p$  capture.

In the beginning of this section we estimated the neutrino transition magnetic moments and SN magnetic fields which are necessary for appreciable  $\nu_e \rightarrow \bar{\nu}_e$  conversions to take place. These estimates were obtained assuming that the relevant RSFP adiabaticity parameters satisfy  $\kappa_{\text{RSFP}} = 1$ , which corresponds to the transition probability of about 80%. Therefore for these values of the neutrino magnetic moments and SN magnetic fields the above estimates of the expected numbers of  $\bar{\nu}_e$  events have to be reduced by the factor 0.8. On the other hand, if, say, 30  $\bar{\nu}_e$  events in Super-Kamiokande can be considered as a clear and unambiguous signal, the requisite values of the transition magnetic moments will be reduced by a factor of 5 (8) for the normal (inverted) neutrino mass hierarchy as compared to our previous estimates. Future very large SN neutrino detectors would have an even better sensitivity to neutrino magnetic moments and SN magnetic fields.

To conclude, the  $\nu_e \rightarrow \bar{\nu}_e$  conversion of supernova neutrinos due to the combined action of neutrino flavor mixing and transition magnetic moments can lead to an observable signal of the neutronization neutrinos in the  $\bar{\nu}_e$  channel. Such an effect would have a clear experimental signature and its observation would be a smoking gun evidence for the neutrino transition magnetic moments. It would also signify a relatively large leptonic mixing parameter  $|J_{e3}| = s_{13} > 10^{-2}$ .

Note added. While this paper was in preparation, the papers [19, 20] appeared in which the  $\nu_e \rightarrow \bar{\nu}_e$  conversions of the supernova neutronization neutrinos were also considered. In the case of the inverted mass hierarchy, our conclusions essentially coincide with those in [19, 20]; however, the authors of those papers did not take into account the RSFP-E and RSFP-X resonances and therefore missed the possibility of a strong  $\nu_e \rightarrow \bar{\nu}_e$  conversion in the case of the normal neutrino mass hierarchy, which was studied in the present paper.

Acknowledgments. The authors are grateful to Alexei Smirnov for useful discussions. TF acknowledges the hospitality of the Abdus Salam International Centre of Theoretical Physics, Trieste, where this work was initiated.

## References

- [1] H. Suzuki, Supernova Neutrinos. In *Physics and Astrophysics of Neutrinos*, ed. by M. Fukugita and A. Suzuki, Springer Verlag, 1994, p. 763.
- [2] A. S. Dighe, A. Y. Smirnov, *Phys. Rev. D* 62 (2000) 033007 [[hep-ph/9907423](#)]; C. Lunardini and A. Y. Smirnov, *Nucl. Phys. B* 616 (2001) 307 [[hep-ph/0106149](#)]; C. Lunardini, A. Y. Smirnov, *JCAP* 0306 (2003) 009 [[hep-ph/0302033](#)]; A. S. Dighe, M. T. Keil, G. G. Raelt, *JCAP* 0306 (2003) 006 [[hep-ph/0304150](#)]; K. Takahashi et al., [hep-ph/0306056](#); I. Gil-Botella, A. Rubbia, [hep-ph/0307244](#).
- [3] S. P. Mikheev, A. Y. Smirnov, *Sov. J. Nucl. Phys.* 42 (1985) 913 [*Yad. Fiz.* 42 (1985) 1441]; L. Wolfenstein, *Phys. Rev. D* 17 (1978) 2369.
- [4] T. A. Thompson, A. Burrows, P. A. Pinto, *Astrophys. J.* 592 (2003) 434 [[astro-ph/0211194](#)].
- [5] J. Schechter, J. W. Valle, *Phys. Rev. D* 24 (1981) 1883 [Erratum *ibid.* D 25 (1982) 283].
- [6] L. B. Okun, M. B. Voloshin, M. I. Vysotsky, *Sov. Phys. JETP* 64 (1986) 446 [*Zh. Eksp. Teor. Fiz.* 91 (1986) 754].
- [7] C. S. Lim, W. J. Marciano, *Phys. Rev. D* 37 (1988) 1368.
- [8] E. K. Akhmedov, *Sov. J. Nucl. Phys.* 48 (1988) 382 [*Yad. Fiz.* 48 (1988) 599].
- [9] E. K. Akhmedov, *Phys. Lett. B* 213 (1988) 64.
- [10] E. K. Akhmedov, Z. G. Berezhiani, *Nucl. Phys. B* 373 (1992) 479.
- [11] H. Athar, J. T. Peltoniemi, A. Y. Smirnov, *Phys. Rev. D* 51 (1995) 6647 [[hep-ph/9501283](#)]; E. K. Akhmedov, A. Lanza, S. T. Petcov and D. W. Sciama, *Phys. Rev. D* 55 (1997) 515 [[hep-ph/9603443](#)]; T. Totani, K. Sato, *Phys. Rev. D* 54 (1996) 5975 [[astro-ph/9609035](#)]; H. Nunokawa, Y. Z. Qian, G. M. Fuller, *Phys. Rev. D* 55 (1997) 3265 [[astro-ph/9610209](#)]; H. Nunokawa, R. Tomas, J. W. Valle, *Astropart. Phys.* 11 (1999) 317 [[astro-ph/9811181](#)]; S. Ando and K. Sato, *Phys. Rev. D* 67 (2003) 023004 [[hep-ph/0211053](#)]; S. Ando and K. Sato, *Phys. Rev. D* 68 (2003) 023003 [[hep-ph/0305052](#)].
- [12] F. J. Botella, C. S. Lim, W. J. Marciano, *Phys. Rev. D* 35 (1987) 896.

- [13] E. K. Akhmedov, C. Lunardini, A. Y. Smirnov, Nucl. Phys. B 643 (2002) 339 [hep-ph/0204091].
- [14] SNO Collaboration, S. N. Ahmed et al, nucl-ex/0309004; G. L. Fogli et al, hep-ph/0308055; The Super-Kamiokande Collaboration, M. B. Smy et al, hep-ex/0309011.
- [15] E. K. Akhmedov, Sov. Phys. JETP 68 (1989) 690 [Zh. Eksp. Teor. Fiz. 95 (1989) 1195].
- [16] E. K. Akhmedov, S. T. Petcov, A. Y. Smirnov, Phys. Rev. D 48 (1993) 2167 [hep-ph/9301211].
- [17] R. C. Duncan, C. Thompson, Astrophys. J. 392 (1992) L9; G. Kouveliotou et al, Nature 393 (1998) 235; D. L. Kaplan et al, astro-ph/0103179.
- [18] P. Vogel, J. F. Beacom, Phys. Rev. D 60 (1999) 053003 [hep-ph/9903554].
- [19] A. Ahriche, J. M. Minouni, astro-ph/0306433.
- [20] S. Ando and K. Sato, hep-ph/0309060.